Proc. Natl. Acad. Sci. USA
Vol. 88, pp. 8592–8596, October 1991
Cell Biology

Distinct pathways for basolateral targeting of membrane and secretory proteins in polarized epithelial cells

(Madin–Darby canine kidney cells/constitutive secretion/polar sorting/microtubules)

WERNER BOLL*†, JACQUELINE S. PARTIN‡, ADRIAN I. KATZ§, MICHAEL J. CAPLAN¶, AND JAMES D. JAMIESON*

*Departments of Cell Biology and ¶Cellular and Molecular Physiology, Yale University School of Medicine, 333 Cedar Street, P.O. Box 3333, New Haven, CT 06510-8002; ‡Department of Pediatrics, State University of New York at Stony Brook, Stony Brook, NY 11794-8111; and §Department of Medicine, University of Chicago, Chicago, IL 60637

Communicated by Vincent T. Marchesi, June 26, 1991

ABSTRACT **Polarized epithelial cells target distinct sets of membrane and secretory proteins to their apical and basolateral domains. Here we examine whether constitutively secreted and membrane proteins that are bound for the same domain share the same carrier vesicles. To address the issue, differential effects of microtubule depolymerization on basolateral protein targeting in the polarized Madin–Darby canine kidney II cell line were studied. We find that the basolateral insertion of the active, ouabain-binding Na^+,K^+-ATPase and of a set of very late antigen integrins is little affected by microtubule disruption. Under equivalent conditions, the basolateral secretion of the basement membrane protein laminin is strongly suppressed. More specifically, it is demonstrated that microtubules are involved in targeting laminin, but not integrins, from the compartment related to the accumulation of newly synthesized proteins at 20°C (trans-Golgi network) to the basolateral domain. Our study also reveals that laminin associated with basolateral binding sites interacts with those sites only secondarily to secretion. The data provide evidence for a branch in the basolateral targeting pathway, with secreted and membrane proteins loaded into distinct carrier vesicles.**

Filter-grown Madin–Darby canine kidney (MDCK) II cells provide a model system for exocytic sorting of proteins (1, 2). In this system, proteins are presumed to be sorted during passage through the trans-Golgi network (TGN) from where they are vectorially targeted to the appropriate surface domains (2). This sorting pattern has previously been shown for a large number of proteins, including the secreted basement membrane proteins laminin and heparan sulfate proteoglycans (HSPG), which are targeted to the basolateral membrane domain of MDCK cells (3). Among the few well-characterized membrane proteins in MDCK cells, Na^+,K^+-ATPase may be sorted to both cell poles (4), although enzymatically active Na^+,K^+-ATPase appears at the basolateral domain only (5). In this study, we examine very late antigen (VLA) (β_1 subunit) integrins, which are potential receptors for basement membrane proteins (6, 7), as a paradigm for vectorial targeting of endogenous membrane proteins to the basolateral cell domain.

It is believed that polarized Golgi-to-surface protein transport uses distinct carrier vesicles to each surface domain (8), but that no further heterogeneity exists among such vesicles (9). The observations we report suggest that vesicular subspecialization, based on carrier loads, may exist.

MATERIALS AND METHODS

Antibodies. Rabbit anti-β_1 antibody against a 39-amino acid synthetic peptide from the C terminus of chicken integrin β_1 subunit was a gift of R. Hynes (Massachusetts Institute of Technology, Cambridge, MA). Anti-ouabain antibody was from D. Louvard (Pasteur Institute, Paris) and B. Rossi (Unité Inserm, Nice, France). Polyclonal rabbit anti-laminin antibodies were from Calbiochem or GIBCO, monoclonal anti-β-tubulin antibody was from Boehringer Mannheim, and fluorescein-conjugated goat anti-mouse antibody was from Kirkegaard and Perry Laboratories (Gaithersburg, MD).

Cell Culture. MDCK II cells were grown on polycarbonate filters in Transwell inserts (pore size, 0.4 μm; diameter, 24 mm; Costar). Plating density was 5×10^5 cells per filter; fresh medium [Dulbecco's modified Eagle's medium (DMEM)/10% fetal calf serum (FCS)/penicillin/streptomycin] was added daily. MDCK II cells were from J. Stow (Harvard University, Cambridge, MA).

Immunocytochemistry. MDCK II cells, grown on filters for 3 days, were incubated for 3 hr under control conditions at 37°C or in the presence of 10 μM colchicine (Sigma) at 4°C. Cells were fixed according to ref. 10 and analyzed by confocal scanning laser microscopy (Bio-Rad MRC-600).

The microtubule staining pattern in MDCK II cells displayed a typical apical-to-basal arrangement (10) 3 days after plating (see *Results*) with a consistent susceptibility to microtubule disrupters thereafter (data not shown).

Pulse–Chase Experiments. Different pulse–chase protocols were used to demonstrate the impacts of microtubule disrupters on basolateral membrane and secreted proteins (protocol A) and to localize these effects at the level of the distal Golgi (protocol B). MDCK II cells were used 6–7 days after plating.

With protocol A, pulse–chase experiments followed microtubule disruption at 37°C. All incubations were performed with or without microtubule disrupter at the concentrations indicated in the figures. Nocodazole (Sigma) was dissolved in dimethyl sulfoxide (DMSO); the final solvent concentration was 0.1%. Cells were incubated with or without colchicine or nocodazole for 4 hr at 37°C in DMEM/10% FCS to depolymerize microtubules before radiolabeling. After starvation for 30 min in methionine-free Eagle's minimal essential medium (EMEM), Tran^{35}S-label (ICN) was added to the basal medium (0.2–1.2 mCi of ^{35}S per ml; specific activity, >1000 Ci/mmol; 1 Ci = 37 GBq) and incubation continued for 30 min at 37°C. For the Na^+,K^+-ATPase, this was followed by a 90-min chase in EMEM with excess ($\geq 10^5$-fold) unlabeled methionine at 37°C and detection of newly synthesized α subunit of Na^+,K^+-ATPase as described (5). For laminin and integrins, the pulse was followed by surface trypsin

The publication costs of this article were defrayed in part by page charge payment. This article must therefore be hereby marked "*advertisement*" in accordance with 18 U.S.C. §1734 solely to indicate this fact.

Abbreviations: VLA, very late antigen; FCS, fetal calf serum; TGN, trans-Golgi network; sulfo-NHS–biotin, sulfo-*N*-hydroxysuccinimido–biotin; HSPG, heparan sulfate proteoglycan(s); MDCK, Madin–Darby canine kidney.

†To whom reprint requests should be addressed.

treatment for 60 min at 4°C (see below) and a chase of 90 min (EMEM/0.5% FCS) in excess unlabeled methionine at 37°C. In washout experiments, nocodazole was omitted from the chase. The regeneration of microtubules was demonstrated by indirect immunofluorescence (data not shown). Apical and basal media were collected and apical or basolateral surfaces were biotinylated with 0.5 mg of sulfo-*N*-hydroxysuccinimido–biotin (sulfo-NHS–biotin) per ml (11). Cells were then lysed and samples were immunoprecipitated as described below.

With protocol B, newly synthesized proteins were allowed to accumulate in the distal Golgi at 20°C in the absence of drugs. Colchicine was then added to examine its effect on surface targeting during a 37°C chase. The 20°C incubation did not interfere with the integrity of microtubules. In detail, after starvation for 30 min in methionine-free EMEM, cells were pulsed for 20 min at 37°C with Tran^{35}S-label (0.2–2.4 mCi of ^{35}S per ml) in the basal medium followed by a 75-min chase at 20°C (EMEM/excess unlabeled methionine) to accumulate proteins in the TGN. Minor secretion of laminin during the 20°C block was detected only after prolonged accumulation (≥2 hr; data not shown). All subsequent incubations were performed with or without colchicine at the concentrations indicated in the figures. Trypsin treatment of cell surfaces for 60 min at 4°C was as described below. To ensure maximal depolymerization of microtubules in colchicine-treated cells (as in Fig. 1 *D–F*), the incubation at 4°C was extended for another 60 min (EMEM/0.5% FCS). The temperature block was released to 37°C and newly synthesized proteins were chased (EMEM/0.5% FCS/excess unlabeled methionine) for the times indicated. Apical and basal media were collected and cell surfaces were biotinylated (11). After lysis of cells, samples were immunoprecipitated as described below.

Surface Trypsin Treatment. The accessibility to sulfo-NHS–biotin of newly synthesized, radiolabeled laminin and integrins may be compromised by the adhesive meshwork of basement membrane proteins (12). To reduce this type of artefact, monolayers were washed with ice-cold phosphate-buffered saline (PBS), containing 0.1 mM $CaCl_2$ and 1 mM $MgCl_2$ (PBS-CM). For each insert, either the basolateral or the apical surface was treated with trypsin (100 μg per ml of PBS-CM) twice for 30 min at 4°C, while the opposite surface was protected by EMEM/10% FCS. Trypsin inactivation was with EMEM/10% FCS (twice for 15 min each; 4°C) and multiple washes with PBS-CM. All incubations after trypsin treatment were performed in the presence of 0.5% FCS to protect from residual trypsin.

Immunoprecipitation. Media were collected and surface-biotinylated cells were lysed [1% Nonidet P-40 (NP-40)/0.5% deoxycholate/0.1% SDS in PBS, pH 7.4] for >1 hr at 4°C in the presence of 2 mM phenylmethylsulfonyl fluoride/10 mM *N*-ethylmaleimide/20 mM EDTA. Proteins of interest were recovered from the precleared lysate by overnight incubation with antisera at 4°C [rabbit anti-β_1 antibody (13) at 1:300; rabbit anti-laminin antibody at 1:200] and subsequently adsorbed to protein A-Sepharose. After washing, antigens were eluted by boiling in SDS sample buffer. Biotinylated surface proteins were then bound to immobilized streptavidin in 1% NP-40/PBS for >4 hr at 4°C. Eluted antigens were analyzed by SDS/PAGE (14) and autoradiography as indicated.

Monolayer Integrity. Monolayer integrity was assessed by the failure of apically administered sulfo-NHS–biotin (M_r 443) to label basolaterally located integrins. This surface labeling was performed immediately after the final chase at 37°C.

RESULTS

Colchicine Disrupts Microtubules. To assess the efficacy of colchicine treatment, microtubules in filter-grown MDCK II cells were visualized by immunofluorescence under the confocal microscope. Sequential 0.5-μm optical sections were obtained along the *z* axis; Fig. 1 shows sections through basal, middle, and apical regions. Incubated at 37°C, control cells display a dense meshwork of microtubules across the basal portion of the cell. Cables of microtubules rise vertically toward the apex, outlining the cell periphery. Apically, a basket-like array of microtubules is seen. Treatment of cells with 10 μM colchicine at 4°C for 3 hr results in total loss of tubulin-specific signal throughout the basal and middle cell regions. Preservation of the basket-like structure around the apically located centrioles after microtubule disrupters is in accord with refs. 10 and 15; it persists during pharmacological intervention and cold-induced depolymerization at 0°C–4°C (10, 16–18).

Basolateral Membrane Protein Delivery Is Microtubule Independent. Initial studies examined the role of microtubules in delivery of endogenous membrane proteins. Fig. 2*A* shows that the basolateral surface presentation of the ouabain-binding α subunit of Na^+,K^+-ATPase is delayed when cells are preincubated, pulsed, and chased all in the presence of colchicine (up to 50 μM); importantly, no apical diversion is observed. Similarly, membrane insertion of VLA integrins is strictly basolateral under control conditions (Fig. 2*B*). Their polarized surface delivery and distribution is preserved when microtubules are disrupted by 10 μM colchicine. The slowdown of basolateral delivery of VLA integrins in the presence of colchicine (Fig. 2*B*) is mirrored by an equivalent intracellular accumulation of integrins (data not shown). Retardation of membrane protein delivery is likely due to the dispersal of the Golgi upon microtubule depolymerization (18).

Microtubules Are Required for Basolateral Laminin Secretion. Filter-grown MDCK cells target laminin with high efficiency into the basal medium (Fig. 3). When preincubated, pulsed, and chased, all with 10 μM colchicine, basolateral laminin secretion is inhibited without increasing its low apical discharge. An equivalent result is obtained for the sorting of HSPG (data not shown). It is necessary to show that the depressive effect of colchicine on laminin secretion is not due to an increase in basolateral surface binding after secretion. In fact, labeling with the membrane-impermeable probe sulfo-NHS–biotin reveals that the amount of newly synthesized laminin associated with the basal surface is depressed to an extent similar to that of laminin collected from the basal medium after microtubule disruption (Fig. 3, lanes BS). A redistribution of surface-associated laminin to the apical domain beyond the level of the controls was not observed (data not shown). The parallel decrease of total basolateral laminin (secreted and cell associated) following colchicine treatment suggests that association of laminin with binding sites on the basolateral surface is a secondary phenomenon resulting from binding after secretion.

Inhibition of Laminin Secretion After Microtubule Disruption Is Reversible. In contrast to colchicine, depolymerization of microtubules with nocodazole is reversible (19). This enabled us to examine cell viability in terms of tubulin repolymerization and restoration of microtubule-dependent secretion. The inhibition of laminin secretion with a chemically different compound strengthens our argument that the results are due to microtubule depolymerization *per se* rather than drug side effects.

Under control conditions, laminin is targeted to the basolateral domain with high efficiency (Fig. 4). When 15 μM nocodazole is present during preincubation, pulse-labeling, and chase, targeting to the basolateral domain is blocked as with colchicine (see Fig. 3). Removal of nocodazole during the chase partially restores laminin secretion. Since total basolateral laminin secretion is represented by its signals from the basal medium and the basolateral surface, the polarity of targeting also appears to be partially reestablished.

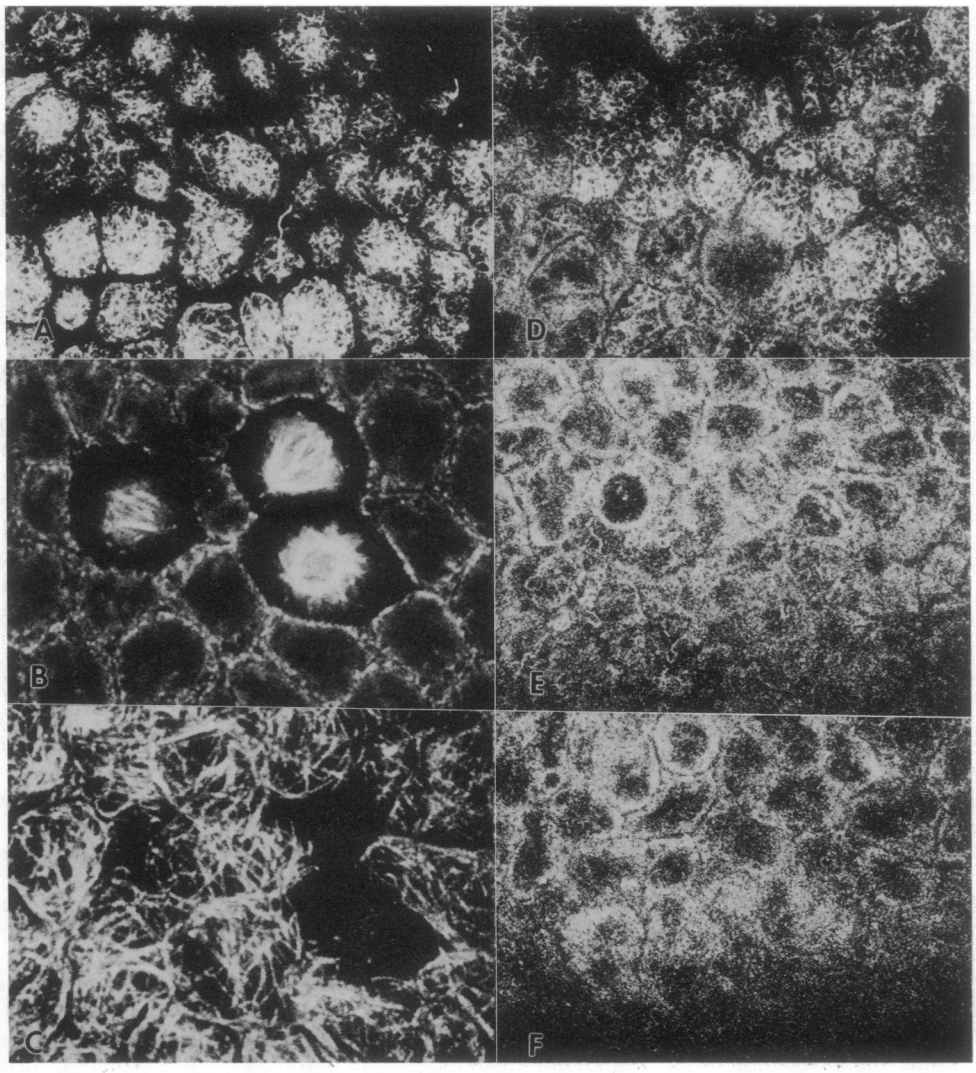

FIG. 1. Immunofluorescence staining of β-tubulin in control and colchicine-treated MDCK II cells. Filter-grown cells, incubated for 3 hr at 37°C (*A–C*) or at 4°C in the presence of 10 μM colchicine (*D–F*) were fixed (10) and labeled with an anti-β-tubulin antibody (1:50). The immunofluorescence signal (fluorescein-conjugated goat anti-mouse; 1:50) was detected by confocal microscopy in optical sections through basal (*C* and *F*), middle (*B* and *E*), and supranuclear apical (*A* and *D*) regions of the cell. Treatment with colchicine at 4°C depolymerizes microtubules in the basal and middle cell regions (*C* and *B* versus *F* and *E*). In the most apical region, only a rarefaction of microtubules is observed (*A* versus *D*). (×375.)

Microtubules Are Essential in Targeting Laminin from the TGN to the Basal Cell Domain. We wished to localize more closely the effects of colchicine within the secretory pathway. Incubation of cells at 20°C results in the accumulation of newly synthesized proteins in the TGN (20, 21). Other studies suggest that the segregation of proteins bound for different destinations occurs in this 20°C compartment (22, 23). If the colchicine effect reflects the segregation of basolateral secretory and membrane proteins into distinct vesicle

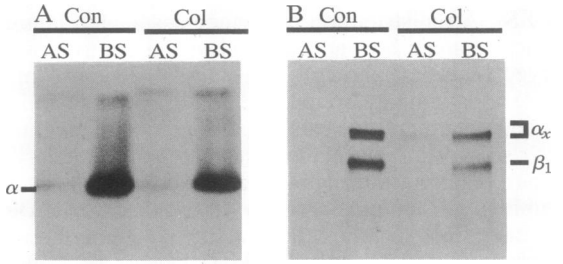

FIG. 2. Depolymerization of microtubules has no major effect on the polar delivery of active Na^+,K^+-ATPase or VLA integrins. AS, apical surface; BS, basolateral surface. Pulse–chase protocol A. (*A*) Using the protocol described (5), the α subunit of active Na^+,K^+-ATPase is inserted basolaterally (Con). This surface distribution is maintained and the quantitative delivery is only slightly decreased when cells are preincubated for 4 hr, pulsed for 30 min, and chased for 90 min with 50 μM colchicine (Col). At 50 μM, colchicine slightly inhibits protein synthesis (≈10%). Autoradiography after SDS/10% PAGE of reduced samples. (*B*) VLA (β_1 subunit) integrins are delivered to the basolateral surface after a 30-min pulse followed by a 90-min chase (Con). When 10 μM colchicine is present during a 4-hr preincubation and the pulse–chase period (Col), the asymmetrical surface distribution is maintained. α_x, Coimmunoprecipitated, uncharacterized VLA α subunits (13). Autoradiography after SDS/5% PAGE of nonreduced samples.

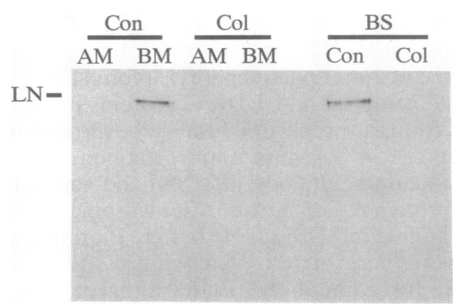

FIG. 3. Depolymerization of microtubules inhibits polar secretion of laminin. AM, apical medium; BM, basal medium; BS, basolateral surface; LN, heterotrimeric laminin. Pulse–chase protocol A. Under control conditions, after a 30-min pulse, laminin is secreted into the basal medium over a 90-min chase with high efficiency (Con). When cells are preincubated for 4 hr, pulse-labeled for 30 min, and chased for 90 min in the presence of 10 μM colchicine, the amount of laminin detected in the basal medium is strongly reduced (Col). An equivalent suppression by colchicine is seen for basolateral cell surface-associated laminin (BS). Autoradiography after SDS/3.5% PAGE of nonreduced samples.

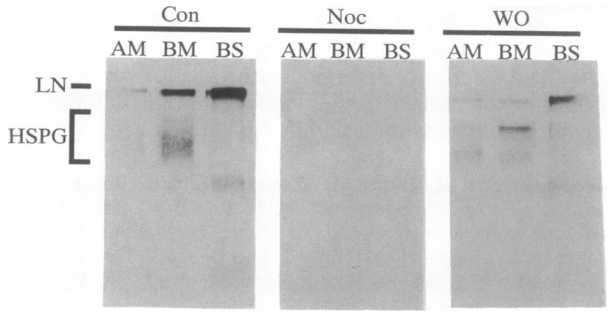

FIG. 4. Effect of microtubule depolymerization on laminin secretion is partially reversible. AM, apical medium; BM, basal medium; BS, basolateral surface; LN, heterotrimeric laminin. Pulse–chase protocol A. After a 30-min pulse, laminin is sorted to the basolateral domain during a 90-min chase with high efficiency (Con). When preincubated for 4 hr, pulsed for 30 min, and chased for 90 min with 15 μM nocodazole, laminin secretion into the basal medium and its association with the basolateral surface are strongly reduced (Noc). When nocodazole is washed out during the 90-min chase, basolateral secretion and surface reassociation are partially restored (WO). HSPG is coimmunoprecipitated by the anti-laminin antibody used. The identities of other coimmunoprecipitated bands are under investigation. Autoradiography after SDS/3.5% PAGE of nonreduced samples.

populations, we would expect the drug to inhibit after sorting in the TGN. To test this hypothesis, we examined the effect of colchicine on laminin that had been preaccumulated at 20°C. This protocol comprises the sequential accumulation of radiolabeled proteins at 20°C in the TGN (20) in the absence of the drug, the depolymerization of microtubules at 4°C in the presence of colchicine (16–18), and the release of the temperature block at 37°C.

The results (Fig. 5) show that colchicine again inhibits basolateral laminin secretion when the protein was recovered from both medium and cell surfaces. Simultaneously, a compensatory apical secretory pathway for laminin and coimmunoprecipitated HSPG is revealed within 30 min and,

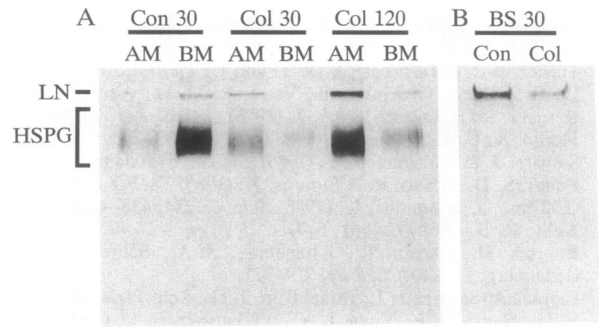

FIG. 5. Basolateral targeting of laminin, following accumulation at 20°C, is inhibited by microtubule disruption. AM, apical medium; BM, basal medium; BS, basolateral surface; LN, heterotrimeric laminin. Pulse–chase protocol B. (*A*) Laminin, preaccumulated at 20°C for 75 min, is predominantly secreted into the basolateral medium after shifting the temperature to 37°C for 30 min (Con 30). HSPG is coimmunoprecipitated by the anti-laminin antibody used. Exposure of cells to 10 μM colchicine for 2.5 hr at 4°C only after accumulation of proteins at 20°C results in an inhibition of basolateral laminin secretion during a 30-min chase at 37°C (Col 30). Increased apical discharge of laminin is now revealed. Apical laminin secretion is more pronounced after extending the chase to 120 min (Col 120). Autoradiography after SDS/3.5% PAGE of nonreduced samples. (*B*) Inhibitory effect of colchicine on secreted laminin, preaccumulated at 20°C, is validated by demonstrating the depressive effect of colchicine on surface-associated laminin during a 30-min chase at 37°C (BS 30). Autoradiography after SDS/3.5% PAGE of nonreduced samples.

more distinctly, during 120 min of chase at 37°C after TGN accumulation and subsequent microtubule disruption. To induce this increase in apical secretion, preaccumulation of proteins at 20°C is necessary but not sufficient. Only the subsequent disruption of microtubules yields partial inversion of laminin secretion shown in Fig. 5. Under the conditions of Figs. 3 and 4 no increase in apical laminin secretion is observed. It should be noted that 10 μM colchicine inhibits neither protein synthesis nor trimerization of laminin (data not shown).

Microtubule Depolymerization Has Little Effect on Golgi-to-Surface Delivery of VLA Integrins. The protocol of 20°C accumulation and subsequent depolymerization of microtubules was used to examine the delivery of TGN-accumulated VLA integrins to the basolateral surface. After a 30-min chase at 37°C, only small quantities of the protein are delivered to the basolateral surface in both the absence and presence of 10 μM colchicine (Fig. 6). No apical diversion was observed (data not shown). After extending the chase to 120 or 180 min at 37°C, VLA integrin delivery to the basolateral surface in control and colchicine-treated cells is apparent (Fig. 6). With this protocol, microtubule disruption appears to slightly retard the delivery of integrins. Under the same conditions, laminin secretion into the basal medium is blocked (Fig. 5). We conclude that the different responses of laminin secretion and integrin delivery to colchicine (cf. Figs. 5 and 6) is attributable to differences in their dependence on microtubules for TGN-to-surface targeting.

DISCUSSION

Recently, many studies have described the importance of microtubules for establishing and maintaining topographical diversity and specificity of transport pathways (16, 24–28). Other than the surface delivery of membrane proteins, however, polarized constitutive secretion and its dependence on microtubules has not been extensively studied. Available results point to an inhibition of apical secretion after microtubule disruption (29, 30). It has also been suggested that common carrier vesicles are used for transporting both membrane and constitutively secreted proteins from the TGN to the plasma membrane (ref. 9, but see ref. 31).

Our report shows that microtubule disruption fails to affect polarized distribution of active Na^+,K^+-ATPase or VLA integrins and has little impact on their delivery to the basolateral surface. This is in keeping with data for membrane proteins in various cell types (15, 17, 27–29, 32). Randomized surface delivery of Na^+,K^+-ATPase in epithelial cells was recently found after domain-selective biotinylation and im-

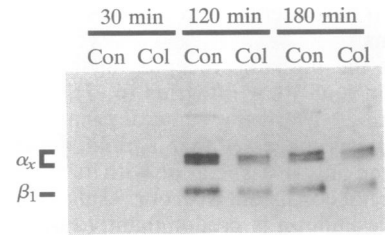

FIG. 6. Basolateral targeting of VLA integrins, following accumulation at 20°C, is only slightly affected by microtubule disruption. Pulse–chase protocol B. After accumulation at 20°C for 75 min, only a small quantity of VLA integrins is delivered to the basolateral surface during a chase of 30 min at 37°C. When the chase at 37°C is extended (120 min, 180 min), the delivery of TGN-accumulated integrins to the basolateral cell surface (Con) is slightly affected by 10 μM colchicine (Col). Under these conditions, laminin secretion is inhibited (see Fig. 5). α_x, A set of uncharacterized, coimmunoprecipitated VLA α subunits (13). Autoradiography after SDS/5% PAGE of nonreduced samples.

munoprecipitation with antibodies to Na^+,K^+-ATPase (4). Nonetheless, our study confirms our previous observations that the α subunit of active Na^+,K^+-ATPase is exclusively inserted postsynthetically into the basolateral domain of MDCK cells (5).

Secretion of laminin shows a complex dependence on microtubules. As we report, the time of initiation of microtubule disruption within a pulse–chase protocol is crucial either in producing inhibition of basolateral laminin secretion (Figs. 3 and 4) or in allowing for compensatory apical discharge (Fig. 5). Although our finding of apical discharge of laminin only under conditions of protein preaccumulation would support the idea of an involvement of microtubules in intra-Golgi transport (28), protein processing in the dispersed Golgi following microtubule disruption (18) needs further study.

While our paper was in review, De Almeida and Stow (33) reported the effects of microtubule disruption on secretion of basement membrane proteins in LLC-PK_1 cells. In an approach similar to our protocol A, these authors find that secretion of both HSPG and laminin is randomized after colchicine pretreatment. Their findings, using indirect immunofluorescence, also complement ours concerning retention of polarity of Na^+,K^+-ATPase after microtubule disruption. Differences in cell lines or variations in experimental protocols may account for the apparent differences between the two studies.

Laminin and basolateral membrane proteins share the common feature of high sorting efficiency toward the basolateral surface, although the underlying mechanisms likely are different. Our study provides strong evidence that only the targeting of laminin toward the basolateral surface depends on intact microtubules. This suggests that membrane and secretory proteins, after being partitioned from the apically directed protein pool, encounter an additional sorting event in the TGN. This step would physically separate basolaterally directed membrane proteins from basolaterally secreted proteins and subsequently load them into distinct carrier vesicles. Our previous findings that acidophilic drugs randomize the sorting of laminin (3) but not of active Na^+,K^+-ATPase (5) bolster this idea (see also ref. 31). The fact that the basolateral cohort of randomly secreted proteins in MDCK and Caco-2 cells is not inhibited by microtubule depolymerization (29, 30) indicates that the requirement for microtubules might be restricted to a subset of proteins that, like laminin, are secreted in a polarized, nonrandom fashion. By analogy with lysosomal proteins (34), they are considered candidates for receptor-mediated sorting (2). Secreted proteins that lack sorting information are postulated to be partitioned with the fluid phase (2) and, unlike laminin, might be loaded into basolaterally directed vesicles carrying membrane proteins.

In view of the probable receptor–ligand relationship between laminin and VLA integrins (6, 7), their segregation during targeting toward the same destination is surprising. Previously, it was suggested that laminin, devoid of a sorting signal, is sorted only in association with its receptor (35). This hypothesis is not consistent with our results, which show that heterotrimeric laminin is predominantly targeted to and secreted from the basolateral surface via carrier vesicles, which are distinct from those bearing integrins. The surface association of laminin apparently results from binding of secreted laminin to membrane receptors (6, 7) or basement membrane components, including prebound laminin itself (12).

In conclusion, a branching sequence of sorting decisions seems to be required to segregate newly synthesized membrane and secreted proteins that will be delivered to and secreted from the basolateral domain. After sorting, proteins are transported in distinct carrier vesicles that differ in their requirement for microtubule integrity. Our results demonstrate the existence of diverging pathways for surface-bound proteins on the basis of carrier load rather than differences of topographical destination within a polarized cell.

We thank Drs. R. Hynes, D. Louvard, and B. Rossi for their generous gifts of antibodies and Dr. J. Stow for kindly providing MDCK II cells. The technical assistance of Philippe Male with confocal microscopy is gratefully acknowledged. This study was supported by U.S. Public Health Service Grants DK 17389, CA 46128 (J.D.J.), and GM 42136 (M.J.C.), the G. Harold and Leila Y. Mathers Charitable Foundation (J.D.J.), and the David and Lucille Packard Foundation (M.J.C.).

1. Caplan, M. J. & Matlin, K. S. (1989) in *Modern Cell Biology*, ed. Satir, B. (Liss, New York), Vol. 8, pp. 71–127.
2. Simons, K. & Wandinger-Ness, A. (1990) *Cell* **62**, 207–210.
3. Caplan, M. J., Stow, J. L., Newman, A. P., Madri, J. A., Anderson, H. C., Farquhar, M. G., Palade, G. E. & Jamieson, J. D. (1987) *Nature (London)* **329**, 632–635.
4. Hammerton, R. W. & Nelson, W. J. (1990) *J. Cell Biol.* **111**, 458 (abstr.).
5. Caplan, M. J., Anderson, H. C., Palade, G. E. & Jamieson, J. D. (1986) *Cell* **46**, 623–631.
6. Hemler, M. E., Huang, C. & Schwarz, L. (1987) *J. Biol. Chem.* **262**, 3300–3309.
7. Sonnenberg, A., Moddermann, P. W. & Hogervorst, F. (1988) *Nature (London)* **336**, 487–489.
8. Wandinger-Ness, A., Bennett, M. K., Antony, C. & Simons, K. (1990) *J. Cell Biol.* **111**, 987–1000.
9. Strous, G. J. A. M., Willemsen, R., van Kerkhof, P., Slot, J. W., Geuze, H. J. & Lodish, H. F. (1983) *J. Cell Biol.* **97**, 1815–1822.
10. Bacallao, R., Antony, C., Dotti, C., Karsenti, E., Stelzer, E. H. K. & Simons, K. (1989) *J. Cell Biol.* **109**, 2817–2832.
11. Le Bivic, A., Real, F. X. & Rodriguez-Boulan, E. (1989) *Proc. Natl. Acad. Sci. USA* **86**, 9313–9317.
12. Martin, G. R. & Timpl, R. (1987) *Annu. Rev. Cell Biol.* **3**, 57–85.
13. Marcantonio, E. E. & Hynes, R. O. (1988) *J. Cell Biol.* **106**, 1765–1772.
14. Laemmli, U. K. (1970) *Nature (London)* **227**, 680–685.
15. Achler, C., Filmer, D., Merte, C. & Drenckhahn, D. (1989) *J. Cell Biol.* **109**, 179–189.
16. Hunziker, W., Male, P. & Mellman, I. S. (1990) *EMBO J.* **9**, 3515–3525.
17. Breitfeld, P. P., McKinnon, W. C. & Mostov, K. (1990) *J. Cell Biol.* **111**, 2365–2373.
18. Turner, J. R. & Tartakoff, A. M. (1989) *J. Cell Biol.* **109**, 2081–2088.
19. De Brabander, M. J., Van de Veire, R. M. L., Aerts, F. E. M., Borgers, M. & Janssen, P. A. J. (1976) *Cancer Res.* **36**, 905–910.
20. Matlin, K. S. & Simons, K. (1983) *Cell* **34**, 233–243.
21. Saraste, J. & Kuismanen, E. (1984) *Cell* **38**, 535–549.
22. Fuller, S. D., Bravo, R. & Simons, K. (1985) *EMBO J.* **4**, 297–307.
23. Griffiths, G. & Simons, K. (1986) *Science* **234**, 438–443.
24. Kelly, R. B. (1990) *Cell* **61**, 5–7.
25. Bomsel, M., Parton, R., Kuznetsov, S. A., Schroer, T. A. & Gruenberg, J. (1990) *Cell* **62**, 719–731.
26. Lippincott-Schwartz, J., Donaldson, J. G., Schweizer, A., Berger, E. G., Hauri, H.-P., Yuan, L. C. & Klausner, R. D. (1990) *Cell* **60**, 821–836.
27. Rindler, M. J., Ivanov, I. E. & Sabatini, D. D. (1987) *J. Cell Biol.* **104**, 231–241.
28. Van Zeijl, M. J. A. H. & Matlin, K. S. (1990) *Cell Reg.* **1**, 921–936.
29. Eilers, U., Klumperman, J. & Hauri, H.-P. (1989) *J. Cell Biol.* **108**, 13–22.
30. Parczyk, K., Haase, W. & Kondor-Koch, C. (1988) *J. Biol. Chem.* **264**, 16837–16846.
31. Hubbard, A. L., Stieger, B. & Bartles, J. R. (1989) *Annu. Rev. Physiol.* **51**, 755–770.
32. Salas, P. J. I., Misek, D. E., Vega-Salas, D. E., Gundersen, D., Cereijido, M. & Rodriguez-Boulan, E. (1986) *J. Cell Biol.* **102**, 1853–1867.
33. De Almeida, J. B. & Stow, J. L. (1991) *Am. J. Physiol.* **260**, C691–C700.
34. Pfeffer, S. R. (1988) *J. Membr. Biol.* **103**, 7–16.
35. Burgess, T. L. & Kelly, R. B. (1987) *Annu. Rev. Cell Biol.* **3**, 243–293.